CFD MODELING OF A CEMENT KILN WITH MULTI CHANNEL BURNER FOR OPTIMIZATION OF FLAME PROFILE

T P BHAD, <u>S SARKAR</u>, A KAUSHIK & S V HERWADKAR

Larsen &Toubro Limited, Mumbai-4000072, India

ABSTRACT

This paper deals with the detailed CFD modelling carried out for a full scale rotary cement kiln with multi channel coal burner. The study includes developing and combining the models of gas-solid flow, modelling of pulverized coal combustion and heat transfer from flue gas to the reacting mass and surroundings. RNG k-ε model for turbulence, eddy dissipation model for coal combustion and P1 radiation model were used in the CFD model.

Effects of geometry modifications for coal burner on flame profile have been studied. The computational models predict the impacts of swirler angle of multichannel coal burner on flame profile, temperature distribution and species concentration studies showed that lower guide vane angle as compared to the existing one result in more intense flame at the centre

KEY WORDS: CFD, multichannel burner, cement kiln, combustion.

NOMENCLATURE:

ε	Dissipation rate of kinetic energy
ϕ	Specific Property, dependent variable
∂	Symbol for Partial Differential
ρ	Density
Γ	Diffusion Coefficient
μ	Dynamic Viscosity
C	Specific heat
D	Mass Diffusion coefficient
∇ (x)	Divergence of the variable x
e	Internal Energy per unit mass
G	Rate of generation of Turbulent Energy
h	Specific Enthalpy
k	Turbulent Kinetic Energy
P	Pressure
S	Volumetric Rate of Heat Generation
T	Static Temperature
t	Time
u, v, w	Velocity Components in the x, y, z directions
x, y, z	Three Spatial directions

INTRODUCTION

Rotary kiln is the key equipment used to produce clinker in cement industry. For design and optimization of rotary kiln, it is necessary to understand the detailed processes that take place in the kiln. It is possible to get more insight, such as the distributions of gas-solid flow, temperature, and composition of gases and particles within a rotary kiln through mathematical modeling. However, only few expressions have existed so far for the processes in a cement rotary kiln to model the fuel combustion, heat transfer, and clinker chemistry. This is owing to the complexity of heat transfer that takes place simultaneously along with chemical and mineralogical reactions. Moreover, the onsite measurements for the detailed physical parameters are complicated and are not possible in many cases. CFD modeling of such a system proves to be beneficial to understand the fluid flow, coal combustion and heat transfer phenomena in rotary kilns, and to improve the efficiency of these units.

Ghoshdastidar and Anandan Unni [1] presented a steady-state heat transfer model for drying and preheating of wet solids with application to one reacting zone of a cement rotary kiln. As per Locher [2,3], conversion ratio of material is linearly dependent on the final temperature at the range between the minimum temperature and the limiting temperature. However, the reaction kinetics was not accounted. CFD predictions for cement rotary kilns including flame modeling, heat transfer, and clinker chemistry were made by Mastorakos et al.,[4,5] in which a comprehensive model for most of the processes occurring in a cement rotary kiln was presented. The results showed potential improvements in the models but only the temperature distribution was given, the gas composition distribution has not been predicted. Shijie Wang, Jidong Lu, et. al [6] presented a heat flux function to take into account the thermal effect of clinker formation. Combining the models of gas-solid flow, heat and mass transfer, and pulverized coal combustion, a set of mathematical models for a full-scale cement rotary kiln were established. In terms of CFD model, gas velocity, gas temperature, and gas components in a cement rotary kiln were obtained by numerical simulation of a 3000 t/d rotary kiln with a four-channel burner. A zone wise heat flux model was presented which accounted for the thermal enthalpy of the clinker formation process and gave more insight to fluid flow, temperature, etc. within the cement rotary kiln.

In the current study, the main objective was to develop a CFD model based on the available plant data for a rotary kiln with multichannel burner to understand the flame profile generated by the burner. Particular objective for this was to carryout an in-depth study of flame profile for creating a more intense flame at the centre of the rotary kiln. Towards this, a comparative study was carried out for the same kiln (along with multichannel coal burner) for four different burner configurations.

PROCESS DESCRIPTION

In a modern dry process cement plant, preheated raw meal from the preheater cyclones enters the precalciner. Precalcined raw material is then fed to the Rotary kiln where a series of physical & chemical process take place to form the clinker. Hot clinker is then led to the cooler. The energy requirement for clinker formation is met by burning fuel (coal, oil, gas) at the lower end of the kiln through multichannel burner. Primary air at ~ 70-80°C is injected from the channels of the burner as swirl & axial air. Secondary air at ~ 1000 °C is drawn from the cooler through the annular opening between burner and the wall of the kiln. Heat transfer between flue gas and charge takes place through radiation and convection. Flue gas from the kiln flows out of the upper end of kiln into the precalciner.

When the raw meal passes through the high temperature zone in the rotary kiln, a series of chemical and mineralogical reactions take place. The components of feed (such as calcium oxide, alumina, ferric oxide, silica, and other metal oxides) interact with each other and finally form four main components of the cement clinker: $3CaO.SiO_2$ (C_3S), $2CaO.SiO_2$ (C_2S), $3CaO.Al_2O_3$ (C_3A), and $4CaO.Al_2O_3.Fe_2O_3$ (C_4AF). The formation temperatures of these clinker components are different. Thus, according to the temperature requirement of different components formed, the dry process rotary kiln can be divided into four zones, namely decomposition zone, transition zone (temperature increasing and exothermal reaction zone), sintering zone, and cooling zone as shown in Figure-1. The thermal effects for the different exothermic and endothermic reactions taking place in the different zones are presented in the Table-1[6].
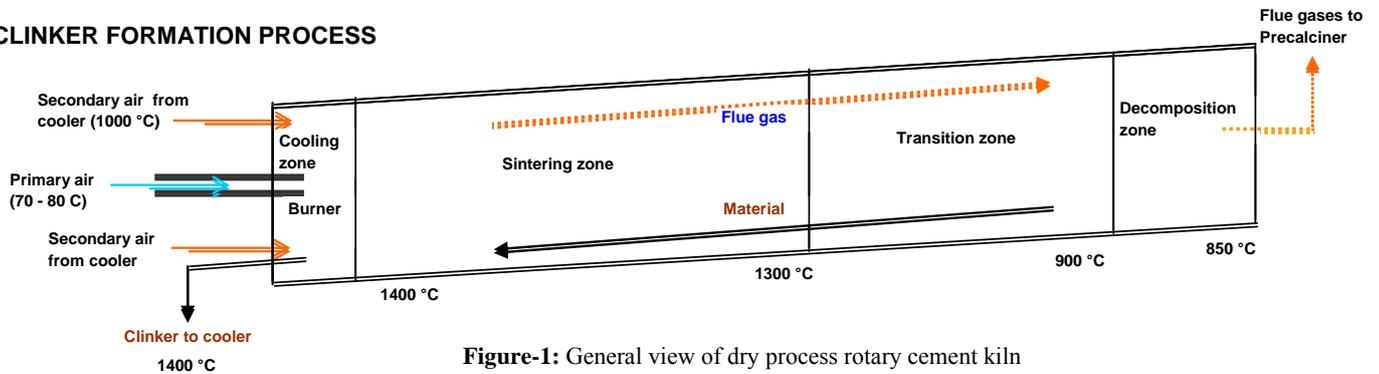
CLINKER FORMATION PROCESS

Figure-1: General view of dry process rotary cement kiln

Reaction Zone	Reaction	Reaction temp. (^{o}C)	Heat of Reaction (ΔH)
Decomposition Zone	$CaCO_3$ decomposition	900	+1660 KJ/Kg of $CaCO_3$
Transition Zone	C_2S formation	900-1300	-603 KJ/Kg of C_2S
Transition Zone	C_4AF formation	900-1300	-109 KJ/Kg of C_4AF
Transition Zone	C_3A formation	900-1300	-37 KJ/Kg of C_3A
Sintering Zone	C_3S formation	1300-1400	-448 KJ/Kg of C_3S

Table 1- Heat of reactions during Clinker formation

MODEL DESCRIPTION

In the current study, based on the available plant data, first a base CFD model for 68 m long, 4.55 m ID rotary kiln along with multichannel coal burner (4500 t/d clinker production capacity) was studied in ANSYS Fluent combining the models of gas-solid flow, heat and mass transfer, and pulverized coal combustion. In the next step, a comparative study was carried out for the same kiln along with multichannel coal burner by changing the vane angle of the swirler of the burner. For modelling the different cases, only vane angle was altered keeping all other modelling aspects same as the base model.

Since the objective was to see the flame profile for the different conditions modelled, it was important to model the heat transfer from flue gas to the reacting mass. However, chemistry of clinker formation, heat transfer from the flue gas to the reacting mass and vice versa etc. have not been modelled in detail. Instead, a similar approach of zone wise heat flux model (after Shijie Wang, Jidong Lu, Weijie Li, Jie Li, and Zhijuan Hu) [6] has been adopted to model the heat transfer from flue gas to surroundings using zone wise overall heat transfer coefficient and reference temperature. Zone wise heat transfer coefficients were in similar proportions as used by Shijie Wang, Jidong Lue et.al. [6], however the absolute values were worked out by trials keeping a tab on the predicted flue gas temperature at the kiln outlet (being the only known parameter as pre plant data). The model included the effects of turbulence on the motion of the coal particles, the radiative heat transfer from the flame to the kiln walls.

On the basis of process analysis and the experiences of design and operation, the proportion of four zones (decomposition zone, transition zone, sintering zone, and cooling zone) in length has been considered as 18:35:41:6 as per the studies carried out by Shijie Wang, Jidong Lue et.al. [6]. The zone wise heat transfer coefficients those were considered in the modelling are presented in Figure-2. In the dry process cement plant, cooling of clinker takes place in cooler and hence length of the cooling zone is kept small in the kiln. For the current modelling, a constant wall temperature of 1400 °C has been considered for the cooling zone.
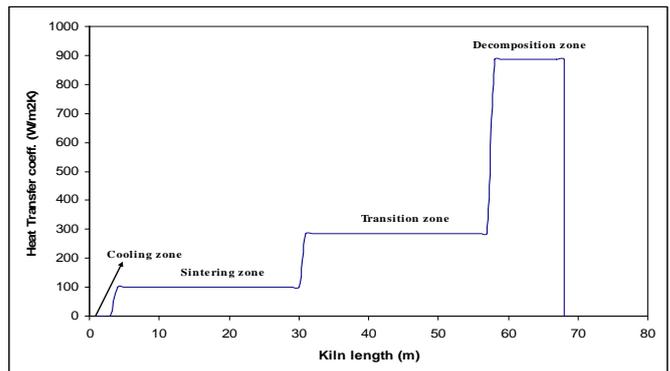

Figure-2: Zone wise heat transfer coefficient for cement rotary kiln

MATHEMATICAL MODEL

The hydrodynamics in a rotary kiln is defined as a gas-solid turbulent flow with chemical reaction. The current model for the rotary kiln consist of RNG k-ε turbulent model for gas phase to capture the swirling effect and particle stochastic trajectory model for solid-phase coupled combustion of volatile and char.

2

Gas Phase Equations

The steady-state continuity and momentum equation of gas phase are given as eqn. 1 & 2. The source term S_p resulted from combustion particles. The components of velocity in coordinate direction x, y, and z are given in eqn. 2, which include pressure, gravitational force (buoyancy effects), and the source term arising from interaction between gas and solid:

Gas phase

$$\frac{\partial}{\partial x_i}\left(\rho u_i\right) = S_p \tag{1}$$

$$\frac{\partial}{\partial x_j}\left(\rho u_i u_j\right) = -\frac{\partial p}{\partial x_i} + \frac{\partial \tau_{ij}}{\partial c_j} + \rho g_i + F_i + S_p \tag{2}$$

The RNG k-ε turbulence model is derived from the instantaneous Navier-Stokes equations, using "renormalization group" (RNG) methods. The analytical derivation results in a model with constants different from those in the standard k-ε model and additional terms and functions in the transport equations for k and ε. The transport equations for the RNG k-ε model are given in eqn. 3 and eqn. 4:

$$\frac{\partial}{\partial x_i}\left(\rho k u_i\right) = -\frac{\partial}{\partial x_j}\left(\alpha_k \mu_{eff} \frac{\partial k}{\partial x_j}\right) + G_k + G_b - \rho\varepsilon \tag{3}$$

$$\frac{\partial}{\partial x_i}\left(\rho\varepsilon u_i\right) = -\frac{\partial}{\partial x_j}\left(\alpha_\varepsilon \mu_{eff} \frac{\partial \varepsilon}{\partial x_j}\right) + C_1 \frac{\varepsilon}{k}\left(G_k + C_3 G_b\right)$$
$$- C_2 \rho \frac{\varepsilon^2}{k} - R_\varepsilon \tag{4}$$

In eqn. 3 and 4, G_k represents the generation of turbulence kinetic energy due to the mean velocity gradients. G_b is the generation of turbulence kinetic energy due to buoyancy. The quantities α_k and α_ε are the inverse effective Prandtl numbers for k and ε, respectively.

The energy equation for solving enthalpy is given in eqn. 5. The source term S_h in the energy equation includes combustion and radiation heat transfer rates:

$$\frac{\partial}{\partial x_i}\left(\rho v_i h\right) = -\frac{\partial}{\partial x_i}\left(\Gamma_h \frac{\partial h}{\partial x_i}\right) + S_h \tag{5}$$

Owing to higher operating temperature in rotary kiln, radiation is the predominant mode of heat transfer. In the current modelling, radiation has been modelled using P1 model of Fluent. The P1 radiation model is the simplest case of the P-N model where the radiation flux, q_r is defined by eqn. 6 as:

$$-\nabla \cdot q_r = aG - 4an^2\sigma T^4 \tag{6}$$

Where, G is the incident radiation, a is the absorption co-efficient, n is the refractive index of the medium and σ is the Stefan Boltzmann constant. The expression for radiation flux can be directly substituted into the energy equation to account for heat sources (or sinks) due to radiation.

Particle phase

Coal combustion has been modeled using the eddy dissipation model of Fluent. The particle phase is treated by solving the Lagrangian equations for the trajectory of a statistically significant sample of individual particle, which represents a number of the real particles with the same properties. In present work, coal particles following a Rossin-Rammler size distribution are tracked in Lagrangian frame of reference using stochastic trajectories model with gravity effect on as shown in eqn. 7 [6].

$$M_p \frac{du_{ip}}{\partial t} = C_D \rho_g \left(\frac{A_p}{2}\right)\left(u_{ig} - u_{ip}\right)\left|u_{ig} - u_{ip}\right| + M_p g_k \tag{7}$$

Combustion processes of coal are treated as de-volatilizing first and then char burning. Combustion of volatile is rapid and the combustion is said to be mixing-controlled, complex, and often unknown, chemical kinetic rates can be safely neglected. FLUENT provides a turbulence-chemistry interaction model (eddy dissipation model), based on the work of Magnussen and Hjertager. The net rate of production of species due to reaction r, $R_{i,r}$, is given by the smaller (i.e., limiting value) of the two expressions below (eqn 8 & 9):

$$R_{i,r} = v'_{i,r} M_{w,i} A\rho \frac{\varepsilon}{k} \min_R\left(\frac{Y_R}{v'_{R,r} M_{w,R}}\right) \tag{8}$$

$$R_{i,r} = v'_{i,r} M_{w,i} AB\rho \frac{\varepsilon}{k} \frac{\sum_p Y_p}{\sum_j^N v''_{j,r} M_{w,j}} \tag{9}$$

Where Y_p, is the mass fraction of any product species, Y_R is the mass fraction of a particular reactant, A is an empirical constant equal to 4.0 & B is an empirical constant equal to 0.5.

In eqn. 8 & 9, the chemical reaction rate is governed by the large-eddy mixing time scale, k / ε, as in the eddy-breakup model of Spalding. Combustion proceeds whenever turbulence is present (k / ε > 0), and an ignition source is not required to initiate combustion.

After the volatile component of the particle is completely evolved, a surface reaction begins, which consumes the combustible fraction, the char, of the particle. The shrinking core model is used to describe the char burning, and the rate is controlled by chemical reaction and oxygen diffusion, given in eqn 10. The kinetic/diffusion-limited rate model assumes that the surface reaction rate is determined either by kinetics or by a diffusion rate. FLUENT uses the model of Baum and Street and Field.

$$\frac{dM_p}{dt} = -A_p P_{ox} \frac{D_o k}{D_o + k} \tag{10}$$

Where where Ap is the surface area of the particle (πd^2), P_{ox} is the partial pressure of oxidant species in the gas surrounding the combusting particle, and the kinetic rate, k incorporates the effects of chemical reaction on the internal surface of the char particle (intrinsic reaction) and pore diffusion. D_o denote the diffusion rate constant.

Process Parameters

The different process parameters considered for the modeling are given below:

Air stream Name		Mass flow rate (kg/s)	Temp. (°C)
Axial air	-	2.88	80
Swirl Air	-	0.509	70
Coal carrier air	-	0.679	70
Secondary air	-	21.97	1050

Coal Feed rate (kg/s)	-	3.72
Min. Particle dia. (mm)	-	1 micron
Max. Particle dia. (mm)	-	250 micron
Mean particle dia (mm)	-	62 micron
No. of Size fractions	-	16
Rosin Rammler spread parameter	-	1.68

Physical properties of coal:

Density	-	1000 kg/m3
Specific heat	-	1100 J/kg-K
Thermal Conductivity	-	0.5 W/mK

Fixed carbon	-	40.2 %
Volatile content	-	22 %

CFD Domain

A 3D modeling has been carried out considering the full geometry of the 68 m long kiln to capture the actual flow phenomena by closely predicting the locations of dead zones, regions of significant pressure drop etc. Burner has been modeled in flushed condition with respect to the kiln outlet. The swirler has been modeled with 8 no. of vanes (Fig-3). Axial air enters the domain through the outermost annular space. Swirl air enters the domain through the concentric annular space and enters the kiln through adjustable opening after attaining swirling motion through the swirler. Pulverized coal along with coal carrier air enters the domain through the annular gap in between the axial air and swirl air. Secondary air enters the domain through the annular space between the burner outer shell and the kiln refractory lining. Details are furnished in Fig-3.
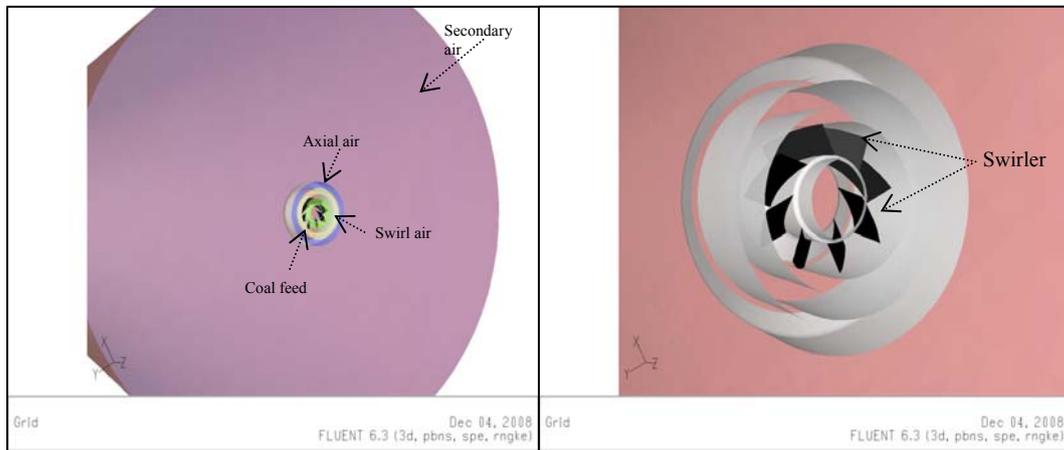

Figure-3 : Burner details
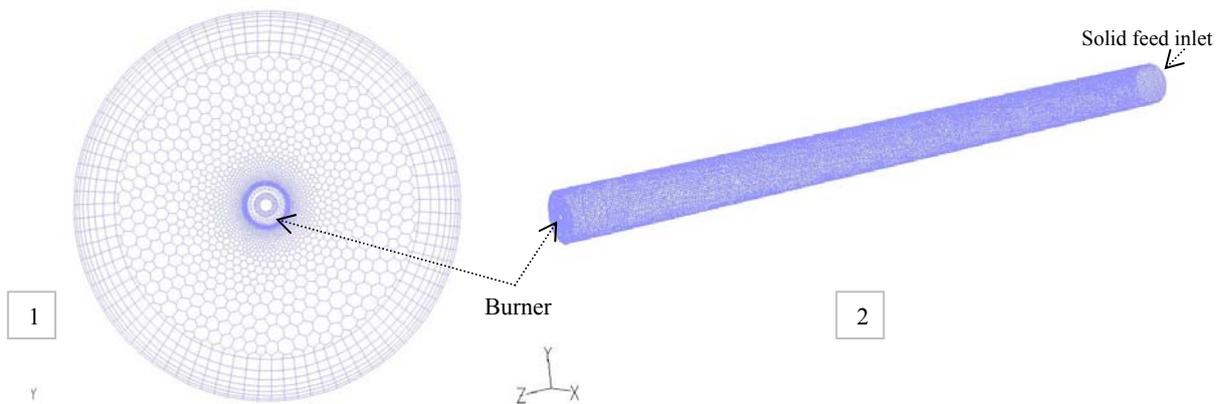
Mesh details

Figure-4 : Mesh details – Surface mesh of (1) Clinker discharge end (2) Full Kiln

A combination of hexahedral and polyhedral cells has been used for meshing. While burner region has been modeled with polyhedra cells, cylindrical shell portion has been modeled with hexahedral elements with five inflation layers. Total number of cells (polyhedral and hexahedral elements) were 442652. Details of the mesh have been shown in Fig-4. Most fine mesh with respect to the available hardware was used for this modelling and further refinement could not be attempted.

Features of the Flow modeling:

Steady state compressible flow with chemical reaction and heat transfer in a 3D domain has been considered. RNG – k ε model has been considered for predicting the reacting high velocity turbulent flow with swirling action. Second order upwind discretization scheme has been used for the convection terms of each governing equation except for pressure where PRESTO has

4

been used to take care of the steep pressure gradients involved in swirling flow at the burner exit. During solution, convergence has been achieved by gradually adding on complexity in the model and carefully adjusting the under-relaxation factors. In addition, rotation of the kiln is neglected and heat transfer coefficient in each zone has been considered to be uniform everywhere.

Boundary Conditions:

Mass flow inlet boundary has been specified at all the inlet boundaries with direction normal to boundary. Coal feed has been defined as combusting particle at coal inlet boundary. All the walls of the kiln, burner, swirler were modeled using as no-slip walls. Heat transfer from flues gases to the reacting mass / kiln walls has been modelled using zone wise heat transfer coefficients on the kiln wall for the decomposition, transition and sintering zones. Additionally for the decomposition zone, a volumetric heat sink has been considered to take care of heat absorption due to the endothermic reaction. Owing to non availability of temperature profile of flue gas along the kiln length, values of the heat transfer coefficients and heat sink have been arrived at through trials by matching the kiln outlet flue gas temperature. For the cooling zone, a constant wall temperature of 1400 °C, corresponding to clinker temperature, has been considered.

Case Studies

Besides the base case (swirler angle 30°) three other burner configurations were modeled with vane angle of the swirler as 22.5°, 37.5° & 45°. Images of the four different vane configurations are presented in Appendix-A. Analysis of the results for the base case study is presented below.

Results & Discussion

Velocity vectors & streamline plots for the different air streams are shown in the Fig-5 & 6. While the axial air comes out of the annular opening as a converging cone at ~ 200 m/s, the swirl air comes out through its opening as a diverging cone with a velocity of ~ 90 m/s. Swirling action of the burner can be seen clearly in the streamline plot. Very intense high velocity re-circulating zone exists in the vicinity of burner which helps in mixing of the pulverized coal with the different air streams. It could also be seen that an entrainment phenomena, i.e., high-temperature secondary air being entrained by high-speed primary air exists in the near-burner region. This is owing to the strong swirl action of the swirl air combined with very high velocity of axial air which acts as a jet and sucks in the secondary air. These phenomena are a benefit to the ignition of coal and the stabilization of flame.
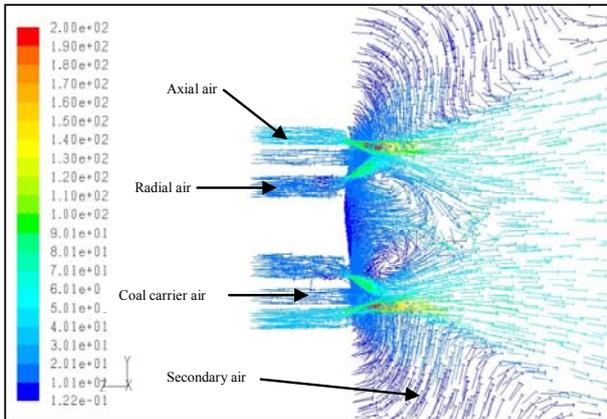

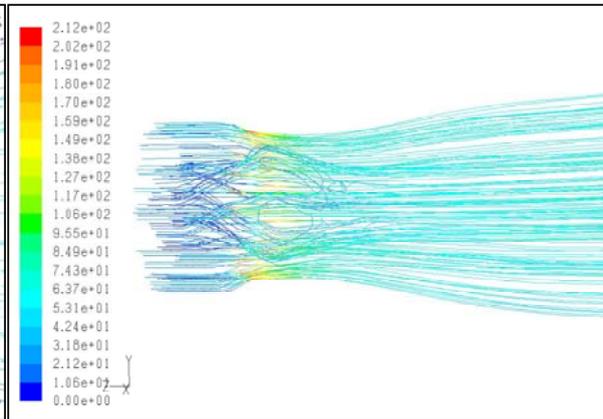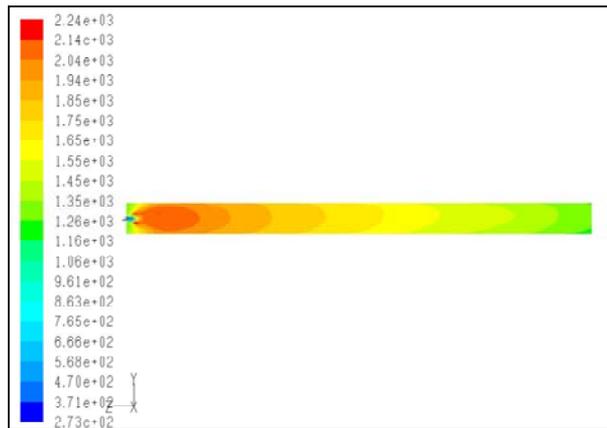Figure-5 : Velocity vector on central plane

Figure-6 : Stream line plot

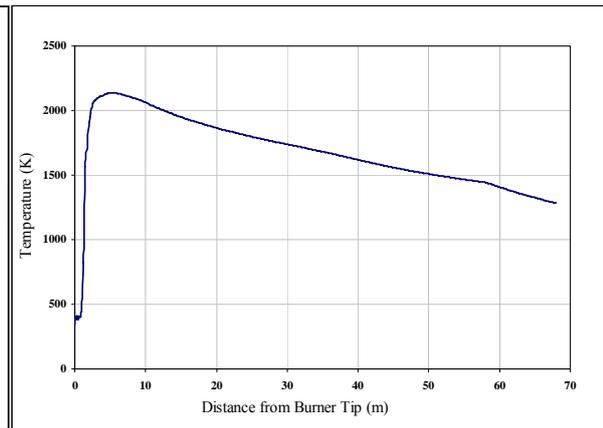

Figure-7: Temperature contour on central plane

Figure-8: Temperature at the centre line along the kiln length
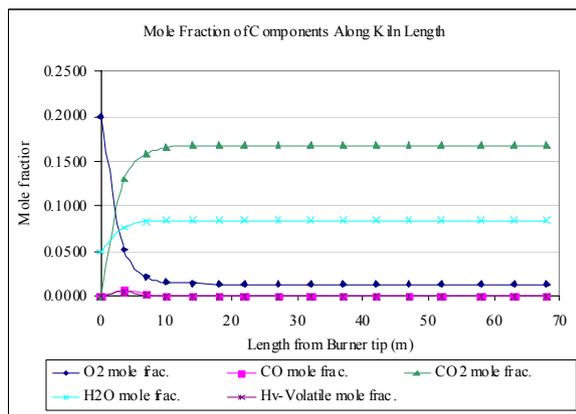
5

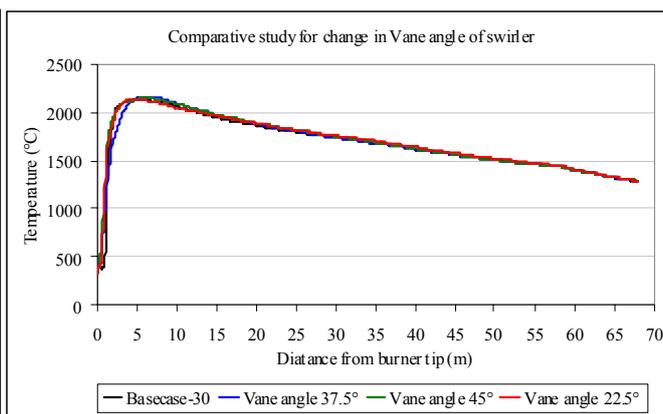Figure-9: Species concentration along the kiln length

Figure-10: Centreline temperature of the kiln for different vane angles

Temperature contours on the mid plane (Fig-7) depicts the shape of flame inside the kiln. Burning of fuel starts ~500 mm away from the burner. Temperature in the flame zone has been predicted to be ~ 2150 K. Flame zone extends up to 12 m from the burner. Flue gas temperature at the kiln outlet has been predicted as 1260 K. Flue gas temperature on central line along the kiln length shown in the graph (Fig-8). At the kiln centre, max. temp. has been observed at 5 m distance from the burner tip.

A summary of mass weighted average mole fractions of components along the kiln length has been presented in Fig.-9. Volatile matter starts evolving at 500 mm from the burner and its combustion starts immediately forming CO_2 & H_2O. This results in sharp depletion of oxygen concentration as the combustion proceeds. Volatile concentration reaches maximum at ~ 1.8 m from burner tip. Generation of CO is linked to volatile combustion and hence follows similar trend as volatile concentration.

Centreline temperatures along the kiln length for the four cases studied (with different vane angles) are presented in Fig-10. From the temperature plots it could be seen that temperature at the centre of the kiln remains almost same for all the four cases beyond 10 m from the burner tip. Small variation in temperature could be seen within 10m distance from the burner tip owing to different flame shapes as shown in Fig-11.
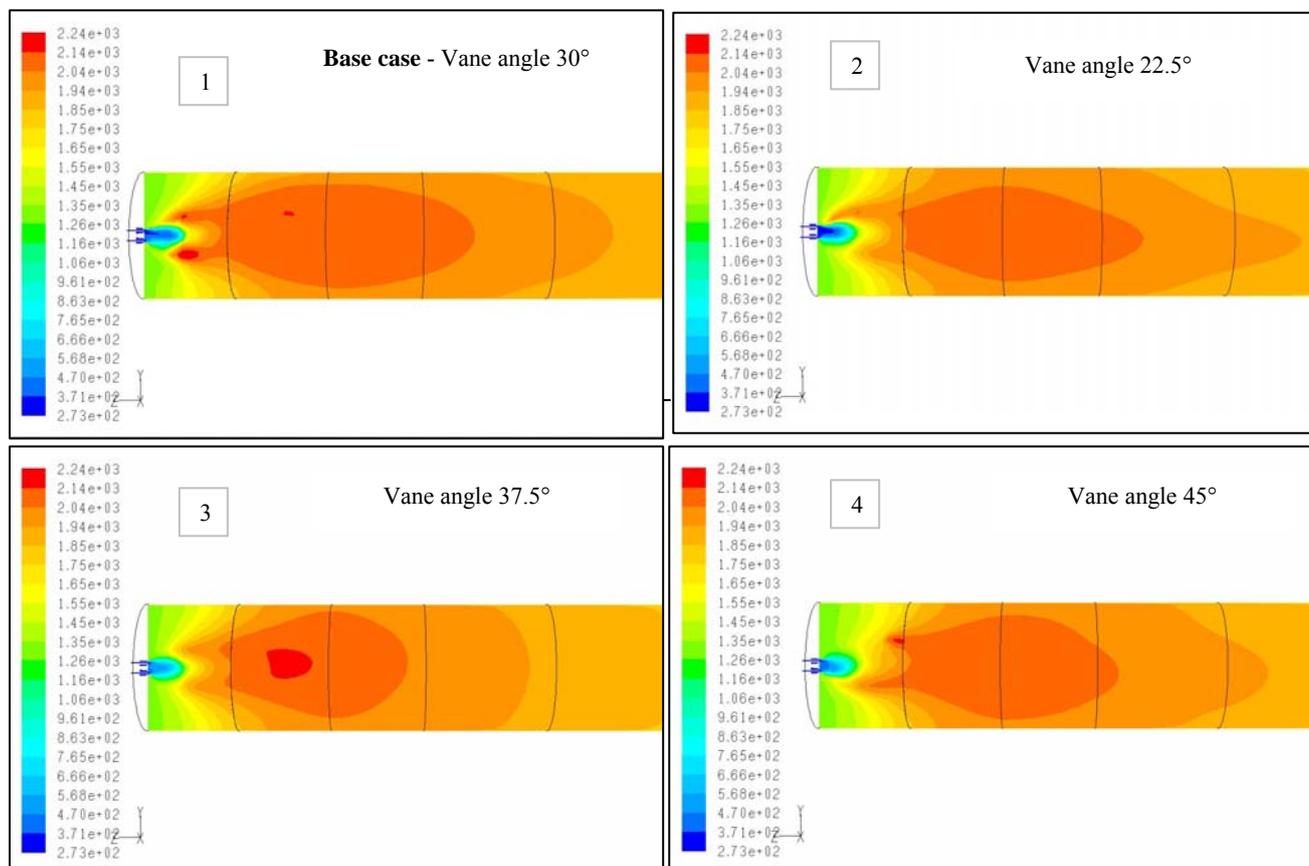

Figure 11: Flame temperature profile for different vane angles (1) Base case-vane angle 30°, (2) Vane angle 22.5°, (3) Vane angle 37.5°,   (4) Vane angle 45°

Temperature profiles on the mid plane for the four different cases studied are presented in Fig-11 and this gives ideas about the flame shapes inside the kiln for the different vane angles. From the Fig-11-1 it could be seen that, for the base case, model predicts flame length of approx. 11 m with flame temperature 2000 – 2150 K. For comparison of results, temperature profiles for the different cases have been plotted in the same temperature sace. With the reduced vane angle of 22.5° (Fig-11-2), flame length remains almost same as the base case with radial contraction of high temperature zone (desirable). For higher vane angle of 37.5° (Fig-11-3), reduction in flame length could be seen, however radial spread of high temperature zone increases. For the highest vane angle of 45° (Fig-11-4), flame length has been predicted to be less than the base case with tendency of spreading the flame in radialially outward indicating the fact that higher vane angle results in spreading of the flame towards the kiln walls which is undesirable. These results need to be validated by experimentation in laboratory / plant.

CONCLUSION

CFD modelling carried out for a full scale rotary cement kiln with multi channel coal burner using commercial CFD code Fluent-6.3.26. The study included developing and combining the models of gas-solid flow and modelling of pulverized coal combustion. Heat transfer model with zone wise heat transfer coefficient accounting for the heat transfer from flue gas to reacting mass and surroundings has been presented.

Four different cases have been studied where the vane angles of the swirler of the burner were varied from 22.5 ° to 45° and impacts of swirler angle on flame profile, temperature distribution and species concentration were predicted. Results indicate that lowering the vane angle from 30 to 22.5° leads to contraction of higher temperature zone radially, which is desirable. With higher vane angle 37.5 & 45°, length of the flame reduces, however, higher temperature zone spreads radially towards the refractory wall. Though changing the vane angles have some effect on flame profile, however, it does not have substantial effect on the overall temperature distribution inside the kiln.
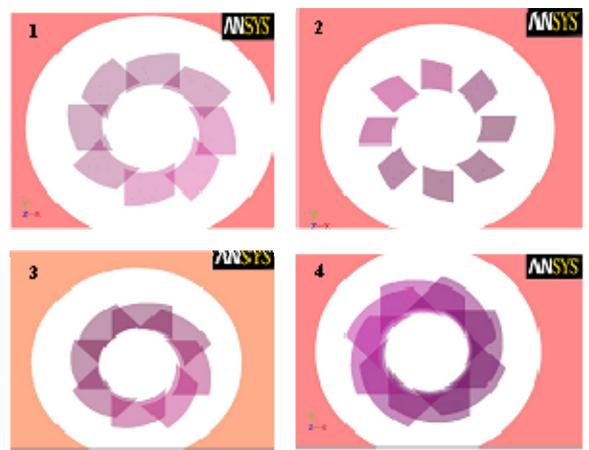
This study gives a direction towards benefit of lower vane angle. However, for the optimum vane angle further studies are needed with validation of results through experimentation.

REFERENCES

1. GHOSHDASTIDAR P. S., ANANDAN UNNI, V. K., (1996), "Heat transfer in the nonreacting zone of a cement rotary kiln", J. Eng. Ind., Trans. ASME, 118 (1), 169-171.

2 LOCHER, G., (2002), "Mathmatical models for the cement clinker burning process. Part 1: Reactions and unit operations", ZKG Int., 55 (1), 29-38.

3. LOCHER, G., (2002), "Mathmatical models for the cement clinker burning process. Part 2: Rotary kiln", ZKG Int., 55 (3), 68-80.

4. MASTORAKOS E., MASSIAS, A., TSAKIROGLOU, C. D., (1999), "CFD predictions for cement kilns including flame modelling, heat transfer and clinker chemistry", Appl. Math. Modelling, 23, 55-76.

5. MASTORAKOS E.,. MASSIAS A., TSAKIROGLOU C.D., (1997), "CFD predictions for cement kilns including flame modeling", Institute of Chemical Engineering and High Temperature Chemical Processes, Foundation for Research and Technology, Greece.

6 SHIJIE WANG, JIDONG LU, WEIJIE LI, JIE LI AND ZHIJUAN HU., (2006),"Modeling of Pulverized Coal Combustion in Cement Rotary Kiln",Jr energy and fuel, vol 20, 2350-2356.

7. "COAL COMBUSTION IN A ROTARY KILN", Application Briefs from Fluent – EX 113

8. MARIA L.S., INDRUSIAK CRISTIANO V. DA SILVA, ARTHUR B. BESKOW AND JOSÉ W. M. KAEHLER., "CFD analysis of the combustion, gas flow, and heat exchange processes in a boiler of a thermal power plant", Energy Production Systems Research Group, Alegre – RS – Brasil, 90619-900.

APPENDIX - A

1 : Vane angle 30° (base case), 2: Vane angle 22.5°
3: Vane angle 37.5°, 4: Vane angle 45°